doi.org/10.36721/PJPS.2026.39.10.278.1

Melatonin attenuates diabetic peripheral neuropathy through modulation of the COX2–IRE1α-mediated endoplasmic reticulum stress axis

Ansong Jin[1] and Leijing Ma[2]*
[1]Departments of Neurology, The First Affiliated Hospital of Kunming Medical University, Kunming 650032, China
[2]Department of Urology, The First Affiliated Hospital of Kunming Medical University, Kunming 650032, China

Abstract: **Background**: Diabetic peripheral neuropathy (DPN) involves Schwann cell injury closely linked to endoplasmic reticulum (ER) stress. Melatonin shows neuroprotective potential, but the specific regulatory mechanisms involving the COX2–IRE1α axis remain to be clarified. **Objectives**: To investigate the potential regulatory role of melatonin in attenuating DPN through the modulation of the COX2–IRE1α ER-stress signaling axis. **Methods**: *In-vitro*, RSC96 Schwann cells were exposed to high glucose (HG) and treated with melatonin (MT), COX2 overexpression, or IRE1α knockdown. Cell viability, apoptosis, and ER stress markers were assessed. *In-vivo*, 30 rats were divided into control, DPN and MT-treated DPN groups (n=10). After 4 weeks of treatment, sensory nerve conduction velocity (SNCV), motor nerve conduction velocity (MNCV), sciatic nerve morphology and protein expression in nerve tissues were analyzed. **Results**: HG significantly reduced cell viability and upregulated ROS and ER-stress markers ($P < 0.05$). MT treatment dose-dependently mitigated these effects. COX2 overexpression partially reversed MT-mediated protection, while IRE1α knockdown attenuated the damage induced by COX2. In DPN rats, 4-week MT treatment significantly improved MNCV and attenuated nerve morphological degeneration compared to the DPN group ($P < 0.05$). MT administration was associated with a significant reduction in COX2 and IRE1α protein expression in sciatic nerve tissue, paralleling the in *vitro* findings. **Conclusion**: Melatonin treatment is associated with improved nerve function and reduced ER stress in DPN models. These protective effects may be mediated via the modulation of the COX2–IRE1α signaling axis, suggesting a potential therapeutic target for DPN.

Keywords: Cyclooxygenase-2 inositol-requiring enzyme 1α; Diabetic peripheral neuropathy; Endoplasmic reticulum stress; Melatonin

Submitted on 16-11-2025 – Revised on 31-03-2026 – Accepted on 13-04-2026

INTRODUCTION

Diabetic peripheral neuropathy (DPN) is a significant microvascular complication among individuals with diabetes, with a notable impact on patient health and quality of life (Jeyam *et al*., 2020; Perveen *et al*., 2024; Selvarajah *et al*., 2019). The therapeutic strategies for DPN mainly include intensive diabetes management and pharmacological treatments targeting its underlying pathogenesis (Ziegler 2023). Current research indicates that disruptions in pathological mechanisms such as oxidative stress, endoplasmic reticulum (ER) stress, neuroinflammatory responses, autophagy and iron metabolism can all contribute to the progression of DPN (Eftekharpour *et al*., 2022; Hagen *et al*., 2021; Patel *et al*., 2023; Yuan *et al*., 2022). Among these mechanisms, ER stress is frequently associated with the accumulation of misfolded proteins in the ER lumen. However, if the stress persists for an extended period or is too severe, the unfolded protein response (UPR) will trigger apoptosis to eliminate the damaged cells (Chen *et al*., 2023).

Melatonin (MT) is an endogenous hormone with potent antioxidant and anti-inflammatory properties and has garnered attention for its role in modulating oxidative stress in diabetic neuropathy (Espino *et al.,* 2019; Shokri *et al.,* 2021). MT has also been found to improve cell function by modulating ER stress-related signaling pathways or interacting with ER-associated sensors. It exerts its mechanisms of action in diseases such as neurodegenerative disorders, cancer and reproductive impairments (de Almeida Chuffa *et al.,* 2024; Xu *et al.,* 2020). Studies have also confirmed that in diabetic neuropathic complications, MT can ameliorate oxidative stress and neurodegenerative damage induced by diabetes, thereby establishing a foundation for the treatment of diabetic neuropathy (Kuthati *et al.,* 2025). In the STZ-induced diabetic mouse model, the role of MT in alleviating neurodegenerative damage occurring throughout the nervous systems has also been confirmed (Che *et al.,* 2020). However, whether MT can participate in the pathogenesis of DPN via the ER stress pathway and the specific molecular mechanisms involved remain to be further investigated.

Prostaglandin-endoperoxide synthase 2 (PTGS2), better known as cyclooxygenase-2 (COX-2), typically exhibits low expression in normal tissues. Its expression is

**Corresponding author:* e-mail: m_leijing3313@163.com

significantly upregulated when cells and tissues are subjected to inflammatory stimuli. It is involved in the pathological processes of inflammation and has been shown to contribute substantially to cancer development, neurodegenerative diseases and inflammation-related disorders (Hashemi Goradel *et al.,* 2019; Yan *et al.,* 2021). Evidence indicates that the expression of this molecule is markedly upregulated in DPN rats, and that reducing COX2 expression can ameliorate damage in high-glucose-induced DPN in *vitro* cell models (Shi *et al.,* 2024b). Inositol-requiring enzyme 1α (IRE1α), one of the three canonical UPR sensors, is a transmembrane protein on the ER with kinase and ribonuclease activities that plays a pivotal role in the UPR (Belyy *et al.,* 2022), Among the UPR branches, IRE1α has been most directly linked to DPN, as its inhibition improves sciatic nerve morphology and function and reduces ER stress-related apoptosis in DPN models (Fridman *et al.,* 2026; Yao *et al.,* 2018b). Mechanistically, COX-2 has been shown to directly bind and activate IRE1α, establishing a molecular link between PTGS2 and ER stress signaling (Groenendyk *et al.,* 2018). In the DPN model, IRE1α is hyperactivated, and its knockdown alleviates ER stress in high-glucose-induced RSC96 cells (Yao. In addition, studies investigating cyclosporine-mediated ER stress and cytotoxicity have found that cyclosporine may affect the ER stress response through the COX-2-IRE1α signaling pathway (Groenendyk *et al.,* 2018). Moreover, selective COX2 inhibitors can suppress ER stress and IRE1α levels in coronary endothelial cells treated with high glucose (Haas *et al.,* 2022). However, whether MT can reduce ER stress in DPN by regulating the COX2/IRE1α axis remains to be investigated. The present work explores the potential of MT to modulate the COX2-IRE1α axis in ER stress-mediated DPN, with the hope of providing a scientific basis for further elucidation of MT's specific molecular mechanisms in DPN therapy.

MATERIALS AND METHODS

Cell culture and treatment

Schwann cells induced by HG were used to establish a DPN cell model (Li *et al.,* 2023). RSC96 (authenticated by STR, CL-0199, Procell, China) were applied for the experiments. The RSC96 cells were allocated into the following groups: Control, HG, low-dose melatonin (HG+MT-L), medium-dose melatonin (HG+MT-M)p, high-dose melatonin (HG+MT-H), HG+MT-H+vector, HG+MT-H+oe-COX2, HG+vector, HG+oe-COX2, HG+oe-COX2+si-NC and HG+oe-COX2+si-IRE1α. The RSC96 cells were cultured in DMEM medium (PM150270, Procell, China) containing 10% fetal bovine serum (FBS, 42F0266K, Gibco, USA), 1% P/S, 4 mM glutamine, 5.5 mM glucose (PB180418, Procell, China), 1 mM sodium pyruvate and 1500 mg/L sodium bicarbonate. Cells were cultured at 37°C with 5% CO_2, with medium changed every 48 hours and passaged at 80% confluence. Control RSC96 cells were maintained in DMEM containing 10% FBS, 5 mL of P/S, and 5.5 mM glucose for 24 hours. HG group cells were exposed to high-glucose medium (10% FBS, 5 mL P/S, DMEM medium + 25mM glucose) for 24 h (Tian *et al.,* 2024). The melatonin treatment groups were treated with 1, 5 and 10 μM melatonin in high-glucose medium for 48 h (Salem *et al.,* 2023), while the Control and HG groups were treated with blank solvent for 48 h. Transfection of relevant vectors into RSC96 cells was performed in high-glucose medium via Lipofectamine® 3000 transfection agent (L3000001, Thermo Fisher, USA). The relevant transfection vectors were synthesized by GeneChem (China).

Plasmid construction and siRNA synthesis

To modulate gene expression, RSC96 cells were transfected with either a mammalian expression vector containing the full-length rat Ptgs2 (COX2) cDNA or specific siRNAs targeting rat Ern1 (Cell Signaling Technology，US), with empty vectors and non-targeting siRNAs (si-NC) serving as negative controls. Transfections were performed using Lipofectamine reagent (*Invitrogen, USA) in Opti-MEM medium according to the manufacturer's instructions, at a final concentration of 2.5 ug of plasmid or 50 nM of* siRNA per well. The culture medium was replaced with fresh complete medium 6–8 h post-transfection.

Detection of cell metabolic activity by CCK-8 assay

To assess cell metabolic activity, a CCK-8 kit (Beijing Jinkelong Biotechnology, China) was employed. Cells were dispensed into 96-well plates (100 μL/well), incubated at 37°C for 24 h with 5% CO_2, treated with 10 μL/well CCK-8, and incubated for 60 minutes. A microplate reader was employed to record absorbance at 450 nm.

Analysis of apoptosis via TUNEL assay

Apoptotic cells were identified with a TUNEL assay kit (MK1013, Boster, China). Cells were fixed on slides and incubated in PBS. After washing, slides were treated with labeling buffer and TUNEL reagents, then incubated at 37°C. They were subsequently blocked and treated with SABC solution to enhance the signal. Finally, slides were counterstained with DAPI (AR1176, Boster, China), mounted and observed employing a fluorescence microscope (CX23, Olympus, Japan).

Detection of ROS levels by DCFH-DA assay

The ROS content was evaluated using the DCFH-DA kit (E-BC-K138-F, Elabscience, China). The cells and tissues from each group were prepared into cell suspensions. Following centrifugation at 1000×g for 5 min, cells were reconstituted in Reagent 1 and incubated at 37°C in the dark for 30 min with intermittent shaking. After washing three times with serum-free medium, cells were resuspended for observation. Integrated optical density was measured with Image Pro Plus software.

Detection of ER stress markers and inflammatory factors by ELISA

The levels of ER stress-associated markers (CHOP, PERK) and inflammatory factors (IL-6, TNF-α) were assessed using commercial ELISA kits (CB10646-Ra, CB12401-Ra, CB10218-Ra, CB11057-Ra, Shanghai Kebiao Biotechnology Co., Ltd., China) For cell samples, cells were collected and washed with PBS, followed by lysis using appropriate lysis buffer to obtain total cellular protein extracts., The lysates were then centrifuged at 12,000 × g for 15 min at 4°C and the supernatants (representing intracellular protein extracts) were collected for ELISA analysis. For tissue samples, tissues were homogenized in cold PBS or lysis buffer and centrifuged at 12,000 × g for 15 min at 4°C. The resulting supernatants were collected for subsequent ELISA assays. All measurements were performed following the kit protocols.

Bioinformatics analysis

The SMILES code of MT was retrieved from the PubChem database and input into the SwissTargetPrediction (2023 version) and TargetNet websites to predict its targets. For SwissTargetPrediction, targets with a probability score > 0 were included, whereas for TargetNet, only targets with a probability score> 0.5 were selected. After deduplication and integration, a total of 147 valid targets of melatonin were obtained. Using the GeneCards database (version 5.16), ER stress-linked genes were screened using the search term “Endoplasmic Reticulum Stress” and only those with a Relevance Score ≥ 7.0 were included to ensure high confidence.

Then, in the GEO database, DPN-related chips were searched and GSE95849 was selected for analysis. The screening criteria for differentially expressed genes were selected based on an adjusted p-value < 0.05 and |logFC| >1. Subsequently, the intersection of MT-related targets, ER stress-related targets and DPN-related targets was performed on the Venn website and the findings were displayed using the Bioinformatics website. The STRING website (version 12.0) was used to analyze protein-protein interactions (PPIs) among the intersecting targets, and the results were visualized in Cytoscape (v3.10.1), with interaction scores calculated.

Detection of COX2 and IRE1α protein expression by western blot

Proteins were extracted using RIPA buffer (89901, Thermo Fisher, USA) and quantified by BCA assay. Western blotting was performed following standard protocols. Membranes were treated with primary antibodies targeting COX2 (1:1000) and IRE1α (2 μg/ml) (ab179800, ab37073, Abcam, UK) overnight at 4°C, followed by incubation with IgG (1:10000) (31466, Thermo Fisher, USA) as secondary antibody for 1 h. Protein expression was detected using a chemiluminescent system and analyzed with ImageJ software, normalized to GAPDH (ab8245, Abcam, UK).

Animal modeling and grouping

Thirty male SD rats, aged 6 weeks and weighing 180–200 g, were obtained from Guangdong Provincial Center for Medical Laboratory Animals (SCXK [Yue] 2022-0002). They were maintained in SPF conditions, fed and watered ad libitum and acclimated for seven days. Approval for this research was granted by the Animal Experiment Ethics Committee of Kunming Medical University (Approval No. kmmu20211525). After a 12-hour fast, 20 SD rats were randomly assigned the model group at random and injected intraperitoneally with streptozotocin (STZ, 60 mg/kg; Shanghai Yuanye Biotechnology Co., Ltd., Cat. No. S17049, purity ≥98.5%). Seventy-two hours later, rats with fasting blood glucose ≥16.7 mmol/L were considered diabetic. These rats were then fed a high-fat/high-sucrose diet (Jilin Seno Biotechnology Co., Ltd., Batch No. 202107250532) for 4 weeks to induce DPN. Electrophysiological assessment was performed at the end of the 4-week modeling period and motor nerve conduction velocity (MNCV) was measured in the sciatic nerve using standard surface stimulation and recording electrodes, comparisons were made between the control and model groups at the same time point.

Successful DPN modeling was defined as an MNCV of <40 m/s (Yu. The 10 rats in the control group were fed a normal diet without STZ injection. The remaining 20 rats with DPN were further randomly assigned to the Model or MT group via a random number table. To minimize potential bias, all outcome assessments, including electrophysiological measurements and histological evaluations, were performed by investigators blinded to group allocation. Control and Model group rats received daily intraperitoneal injections of 10 mL/kg PBS, while those in the MT group received 10 mg/kg MT daily for 4 weeks. All injections were administered between 10:00 and 11:00 am (Pourhanifeh *et al.,* 2020).

Body weight and blood glucose monitoring

Rats had their body weight and blood glucose measured before and during the treatment. During the treatment period, measurements were taken every seven days. Blood glucose was determined by collecting blood from the rat’s tail tip after a 12-hour fast.

Nerve conduction velocity measurement

After the 4week treatment, nerve conduction studies were performed in live rats anesthetized with an intraperitoneal injection of 1% pentobarbital sodium (50 mg/kg) before euthanasia. They were then fixed in a prone position on the experimental table and the sciatic nerve was exposed. For sensory nerve conduction velocity (SNCV) measurement, two recording sites were positioned along the sciatic nerve, and the latency difference (T1) between them was measured following single square-wave stimulation.

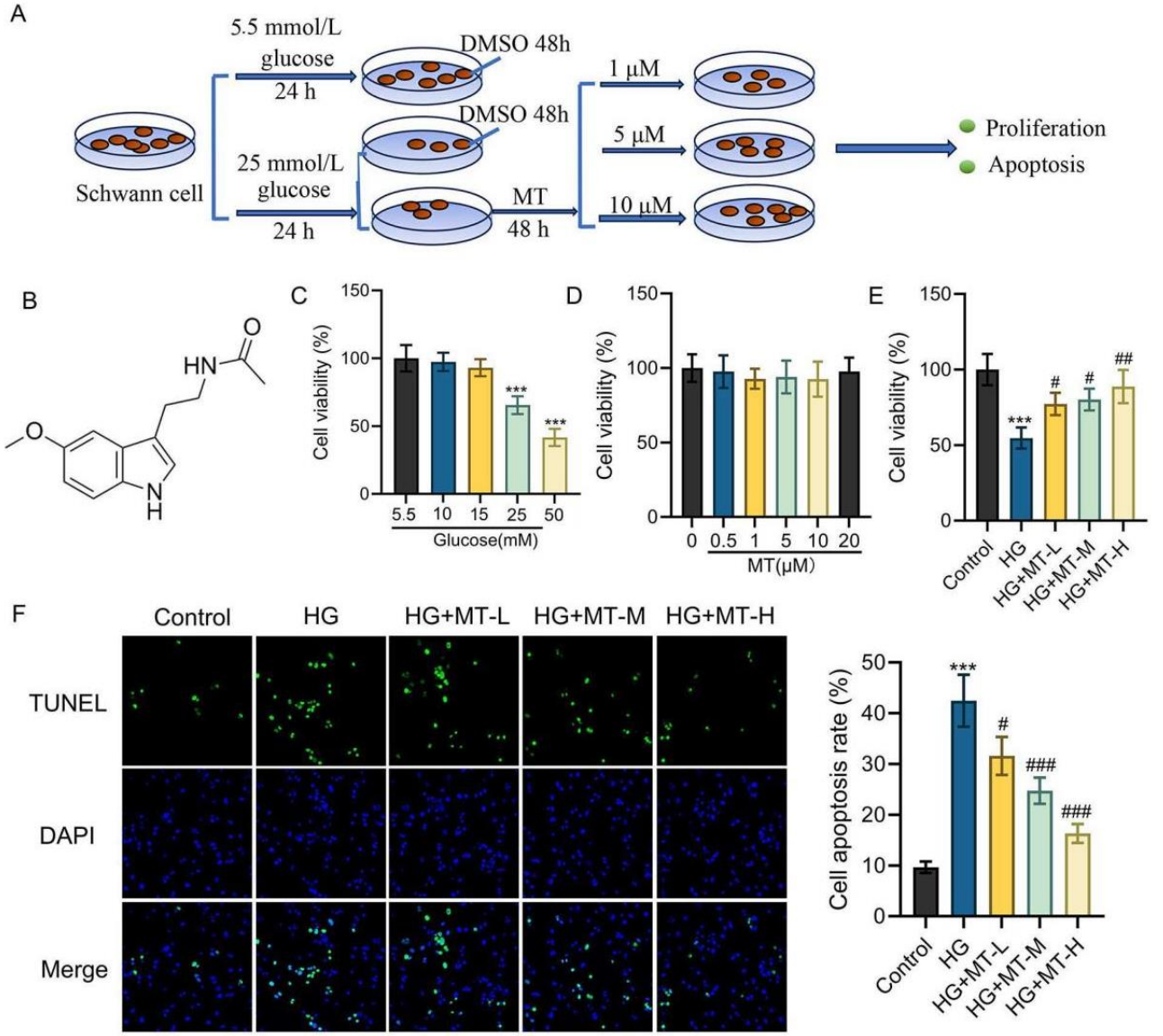

Fig. 1: The effect of MT on HG-induced injury in RSC96 cells.
Notes: A: Schematic diagram of the cell experiment; B: Structural formula of MT; C: The effect of different concentrations of glucose on the viability of RSC96 cells (n = 6); D: The effect of MT on the viability of normal RSC96 cells (n = 6); E: Detection results of cell metabolic activity levels in each group (n = 6); F: Detection results of apoptosis rates in each group (n = 6). ***P<0.001 *vs.* the Control group; #P<0.05, ##P<0.01, ###P<0.001 *vs.* the HG group.

The distance between the two sites (*D*, 1 cm) was measured and conduction velocity was calculated as SNCV = D/T1. (Feng *et al.,* 2025). For MNCV measurement, stimulating electrodes were placed at the efferent portion of the sciatic nerve and recording electrodes were placed at a proximal site. The distance between the two electrodes was recorded as S_2 and the interval between stimulation onset and the emergence of the action potential was noted as the action potential latency (T_2). The MNCV was calculated using the formula MNCV (m/s) = S_2/T_2 (Wang *et al.,* 2020).

Hematoxylin and eosin (HE) staining

Immediately after nerve conduction measurements, the rats were euthanized under anesthesia. The sciatic nerves were dissected and stabilized in 4% PFA. Tissues underwent dehydration, clearing and paraffin embedding. Consecutive 5-μm sections were cut and subjected to staining with HE for histological observation under light microscopy.

Immunohistochemistry

Paraffin-embedded sciatic nerve sections were dewaxed and rehydrated. Following antigen retrieval, sections were treated with 3% H_2O_2 for 10 min at room temperature, then washed with PBS and blocked with goat serum. Primary antibodies against COX2 (2 μg/ml) and IRE1α (1:100)

were applied and maintained at 4°C for 48 h. Following PBS washes, a secondary antibody (IgG, diluted 1:1000) was added and incubated at 37°C for 50 min. Sections were then stained with DAB, mounted and observed under a microscope. The average optical density (AOD) was quantified using Image Pro Plus software.

Statistical analysis

Statistical analysis was performed using SPSS software. Measurement data are presented as mean ±standard deviation ($\bar{x}$±s). When data were normally distributed, one-way ANOVA was performed to compare multiple groups, with subsequent pairwise comparisons via the LSD-t test. For non-normally distributed data, non-parametric analyses were applied. Statistical significance was set as $P<0.05$.

RESULTS

MT inhibits HG-induced RSC96 cell injury

The cell experiment design is shown in figure 1A, with the chemical structure of MT shown in figure 1B. RSC96 cells were exposed to different glucose concentrations (5.5–50 mM) and their viability was measured via CCK-8 assay. Therefore, a glucose concentration of 25 mM was selected for the subsequent high-glucose group to simulate the *in-vitro* cell model (Fig. 1C). The cytotoxic effects of different concentrations (0.5-20 μM) of MT on normal RSC96 cells were detected. The results showed that when MT was ≤20 μmol/L, it had no obvious toxic effects on normal RSC96 cells ($P>0.05$) (Fig. 1D). Furthermore, HG-treated RSC96 cells showed reduced viability and increased apoptosis compared to controls ($P<0.05$), which were reversed by MT treatment ($P<0.05$) (Figs. 1E-F).

MT alleviates ER stress levels in HG-induced RSC96 cells

Under HG conditions, RSC96 cells exhibited significantly higher levels of ROS, CHOP, PERK, IL-6, and TNF-α than controls ($P<0.05$). However, MT administration caused a dose-dependent and pronounced decline in these levels (Figs. 2A-C), suggesting its potential to mitigate inflammation and ER stress in HG-exposed RSC96 cells.

The ameliorative influence of MT on HG-induced RSC96 cells are associated with COX2

A total of 147 MT-related targets were identified using the SwissTargetPrediction and Targetnet websites. The GSE95849 chip identified 6,480 DPN-related targets and 1,519 ER stress-related targets were screened from the GeneCards database. The intersection of MT treatment targets for DPN and ER stress-related targets yielded 19 targets (Fig. 3A). Further PPI analysis of the 19 intersecting targets showed the strongest interaction between PTGS2 (COX2) and other targets (Fig. 3B). Molecular docking results indicated a binding energy of -8.2 kcal/mol between MT and PTGS2 (COX2), representing a favorable theoretical binding affinity and suggesting a potential molecular interaction (Fig. 3C). Therefore, PTGS2, namely COX2, was identified as a primary candidate target for further investigation. Western blot analysis of COX2 protein expression in RSC96 cells revealed that HG significantly increased COX2 levels, while MT intervention markedly suppressed COX2 protein levels (both $P<0.05$) (Fig. 3D).

Overexpression of COX2 reverses the ameliorative effects of MT on HG-induced RSC96 cells

Under HG conditions, RSC96 cells showed decreased viability, increased apoptosis and elevated levels of ROS, CHOP, PERK, IL-6 and TNF-α ($P<0.05$). High-dose MT (HG+MT-H) improved viability, reduced apoptosis and lowered these levels ($P<0.05$). However, COX2 overexpression in the HG+MT-H+oe-COX2 group reversed these effects, reducing viability, increasing apoptosis and raising ROS, CHOP, PERK, IL-6 and TNF-α concentrations ($P<0.05$) (Figs. 4A-E). This suggests that COX2 overexpression may negate MT's protective effects, worsening inflammation and ER stress in RSC96 cells subjected to HG.

Knockdown of IRE1α reverses the damaging effects of COX2 overexpression on HG-induced RSC96 cells

Western blot analysis illustrated that IRE1α expression was significantly higher in the HG group than in controls ($P<0.05$) and further increased in the HG+oe-COX2 group versus the HG+vector group ($P<0.05$) (Fig. 5A). The HG+oe-COX2 group exhibited diminished cell viability, increased apoptosis and elevated levels of ROS, CHOP, PERK, IL-6 and TNF-α relative to the HG+vector group ($P<0.05$). Conversely, in the HG+oe-COX2+si-IRE1α group, cell viability increased, apoptosis decreased and these levels were reduced compared to the HG+oe-COX2+si-NC group ($P<0.05$) (Figs. 5B-F).

Overall, IRE1α knockdown could counteract the detrimental effects of COX2 overexpression in RSC96 cells exposed to HG, enhancing cell viability, dampening apoptosis and alleviating inflammation and ER stress.

MT improves nerve damage in DPN rats

The animal experiment design was shown in figure 6A. Rat body weight increased over time, with comparable values between groups ($P>0.05$) (Fig. 6B). Blood glucose levels remained stable across all groups. Fasting blood glucose was higher in the Model and MT groups than in the Control group ($P<0.05$). Still, no significant difference was observed between the Model and MT groups ($P>0.05$) (Fig. 6B). HE staining revealed pathological changes in rat sciatic nerve tissues: the Control group showed intact nerve fibers and myelin sheaths. In contrast, the Model group exhibited thinner fibers, demyelination and vacuolar degeneration. The MT group showed less nerve damage (Fig. 6C).

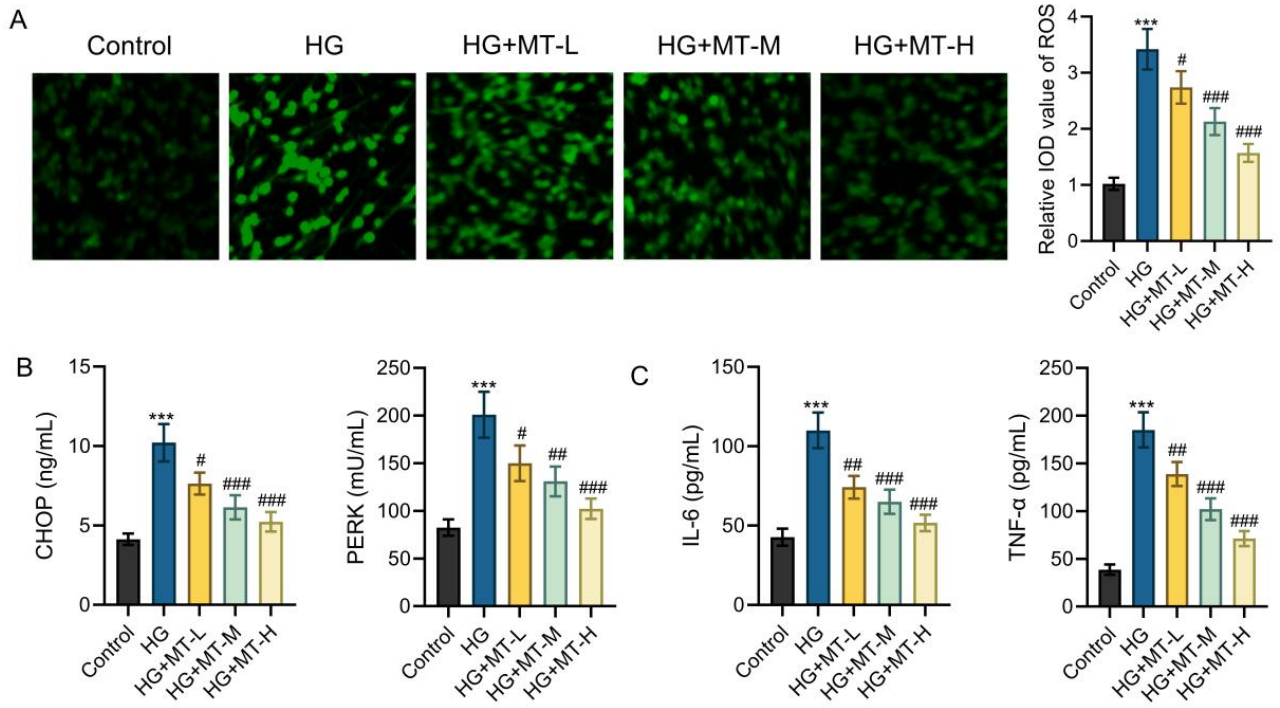

Fig. 2: The effect of MT on ER stress levels in HG-induced RSC96 cells
Notes: A: Detection results of ROS levels; B: Detection results of CHOP and PERK levels (n = 6); C: Detection results of IL-6 and TNF-α levels (n = 6). ***P<0.001 *vs.* the Control group; #P<0.05, ##P<0.01, ###P<0.001 *vs.* the HG group.

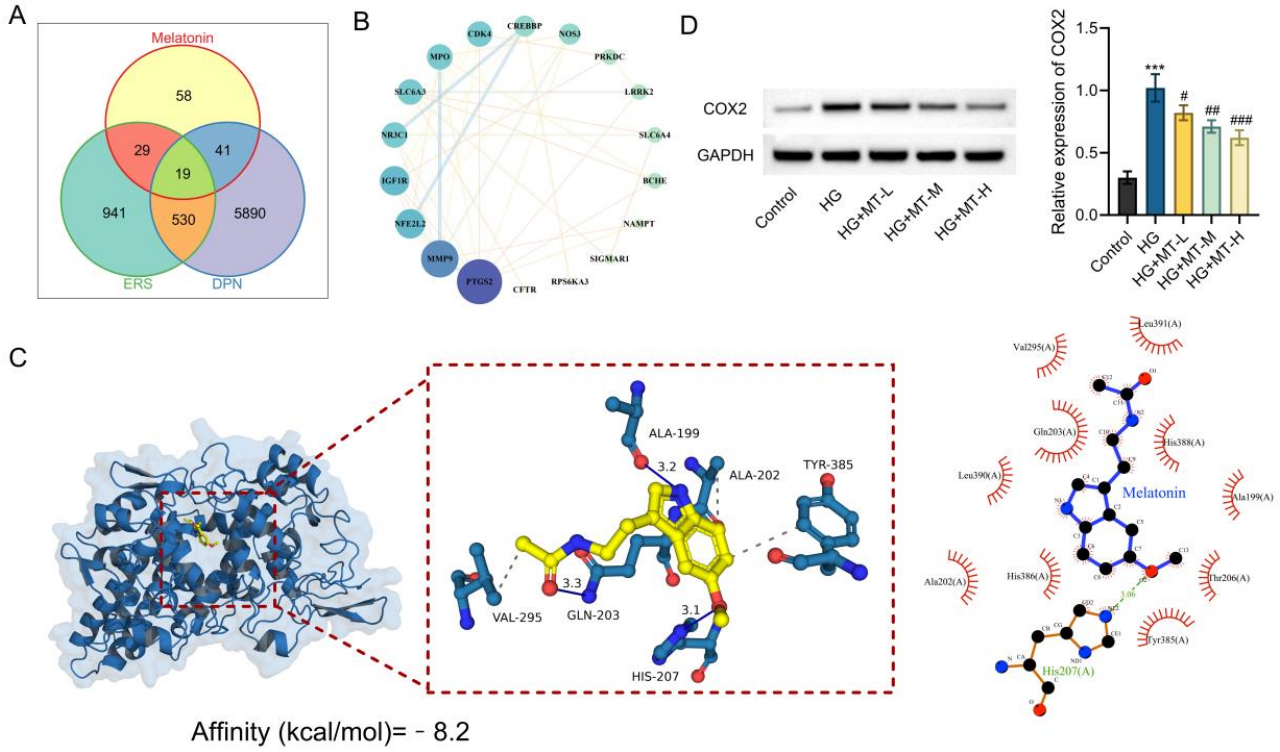

Fig. 3: COX2 is a molecular target of MT
Notes: A: Venn diagram of the intersection of the three sets; B: PPI results; C: Molecular docking results; D: Western blot detection of COX2 expression. ***P<0.001 *vs.* the Control group; #P<0.05, ##P<0.01 *vs.* the HG group.

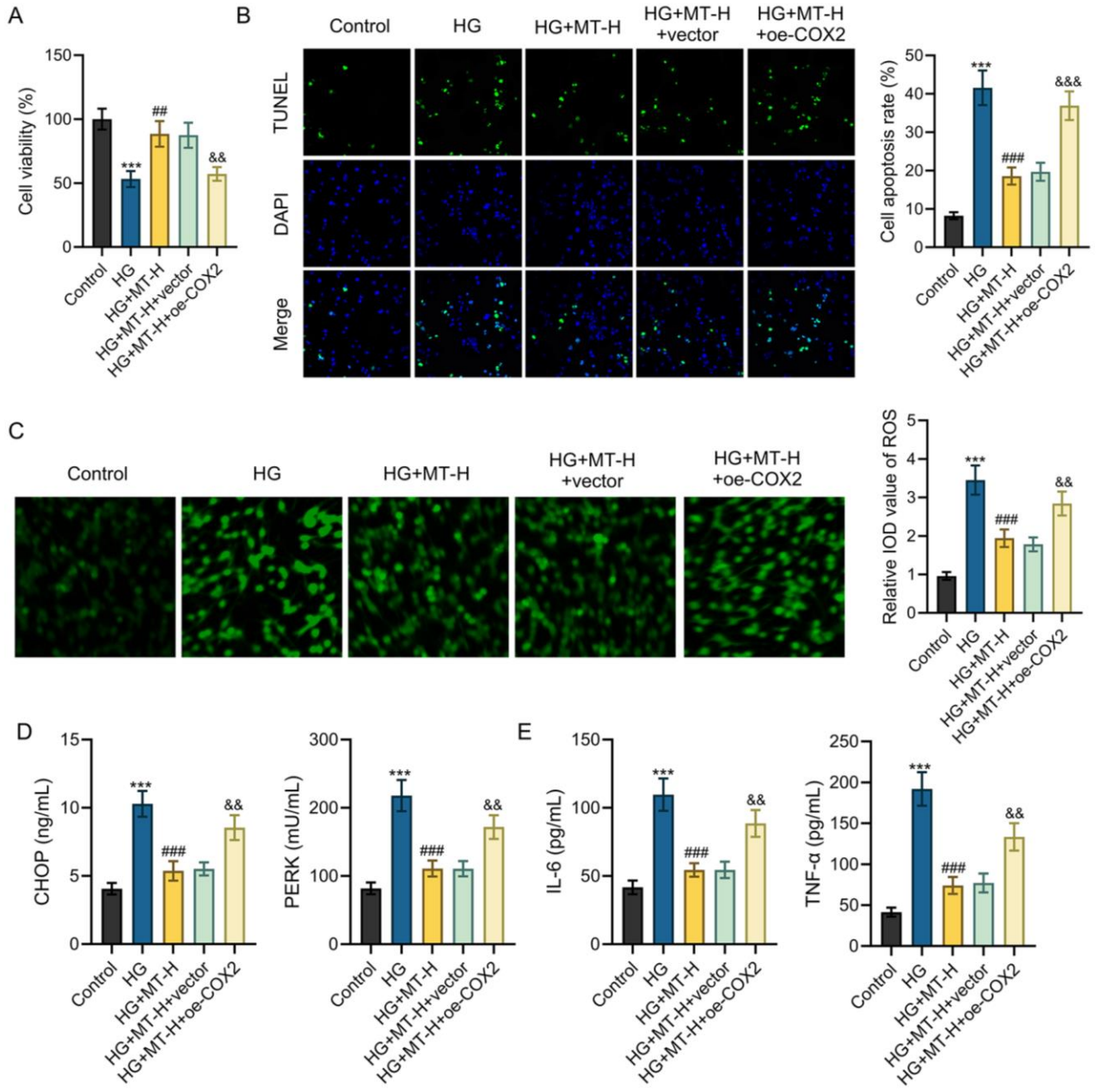

Fig. 4: The effect of COX2 overexpression on HG-induced RSC96 cells
Notes: A: Detection results of cell metabolic activity levels (n = 6); B: Detection results of apoptosis rates (n = 6); C: Detection results of ROS levels (n = 6); D: Detection results of CHOP and PERK levels (n = 6); E: Detection results of IL-6 and TNF-α levels (n = 6). ***P<0.001 *vs.* the Control group; ##P<0.01, ###P<0.001 *vs.* the HG group; &&P<0.01, &&&P<0.001 *vs*. the HG+MT-H+vector group.

The Model group had significantly decreased SNCV and MNCV, elevated ROS, CHOP, PERK, IL-6, TNF-α levels. It upregulated COX2 and IRE1α expression versus the Control group (P<0.05). The MT group exhibited improved SNCV and MNCV, reduced levels of inflammatory and ER stress markers, and downregulation of COX2 and IRE1α relative to the Model group (P<0.05) (Figs. 6D-G). In summary, MT alleviates sciatic nerve damage and ER stress in DPN rats, potentially via the COX2/IRE1α pathway.

DISCUSSION

DPN is a typical distal symmetric polyneuropathy that affects the autonomic, sensory, and motor nerves, leading to significant limb pain and cognitive decline in patients (Chang *et al.,* 2023; Elafros *et al.,* 2022). MT is an indole hormone produced by the pineal gland and other tissues. It has antioxidant and anti-inflammatory effects and shows promise in treating diabetic complications and nerve damage (Ocak *et al.,* 2022).

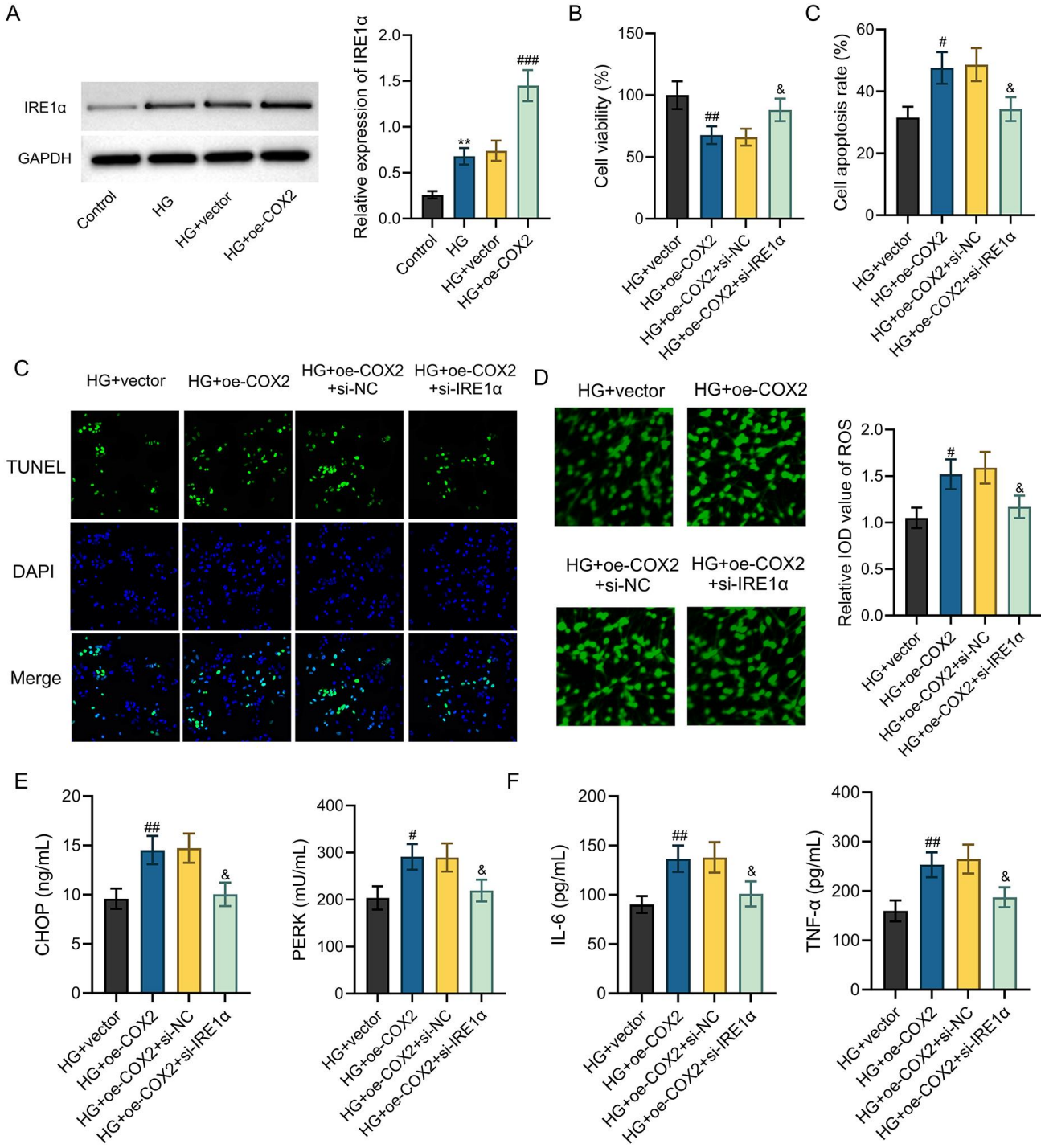

Fig. 5: The effect of IRE1α knockdown on HG-induced RSC96 cells

Notes: A: Western blot detection of IRE1α expression (n = 6); (B) Detection results of cell metabolic activity levels (n = 6); C: Detection results of apoptosis levels; D: Detection results of ROS levels (n = 6); (E) Detection results of CHOP and PERK levels (n = 6); F: Detection results of IL-6 and TNF-α levels (n = 6). **P*<0.05, ***P*<0.01, ****P*<0.001 *vs.* the Control group; #*P*<0.05, ##*P*<0.01 *vs.* the HG+vector group; &*P*<0.05 *vs.* the HG+oe-COX2+si-NC group.

In this study, we constructed an *in vitro cell model using HG-induced RSC96 cells and an in vivo DPN rat model induced by STZ, and treated both* with MT. The results showed that MT effectively alleviated nerve damage in DPN and improvement in the related symptoms.

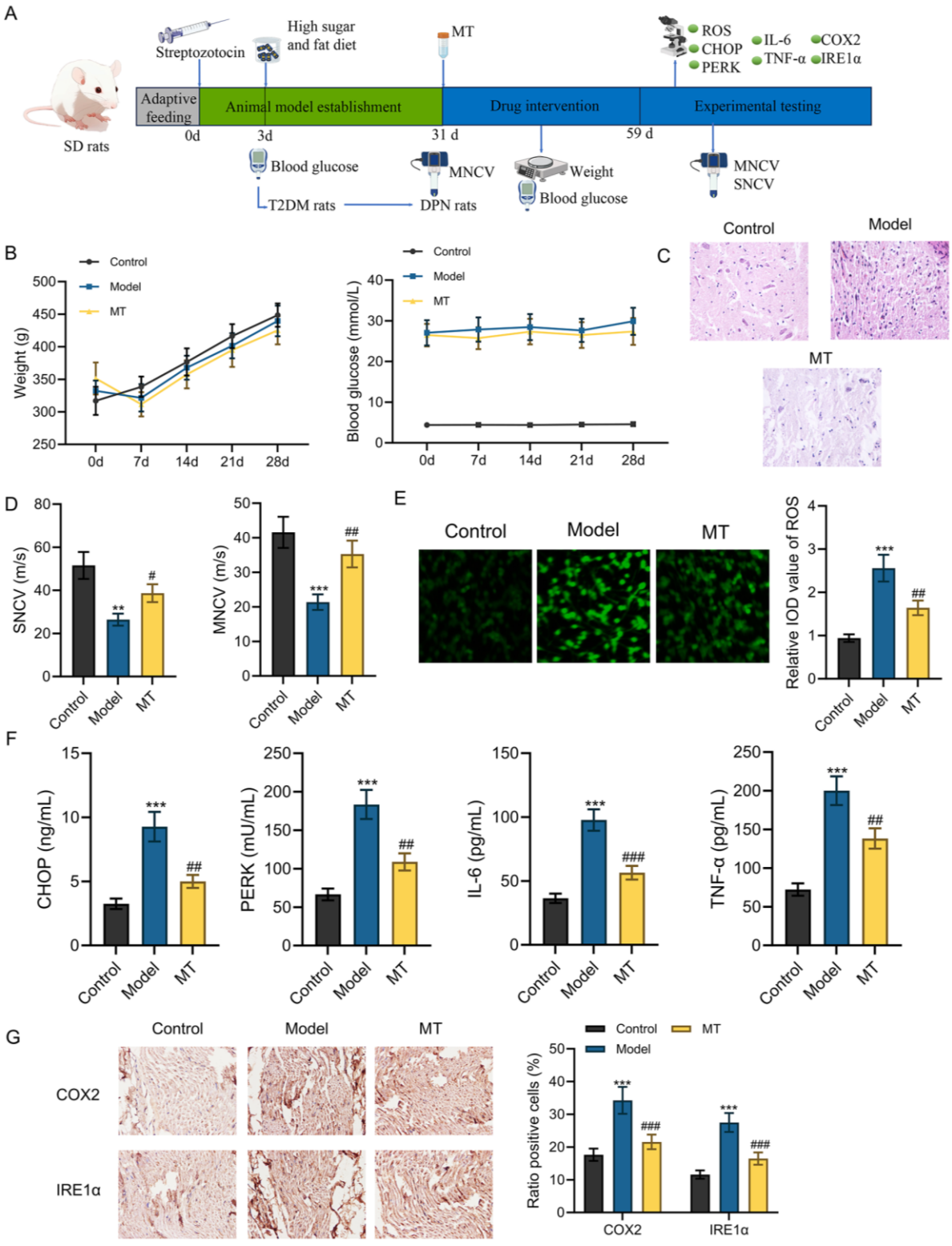

Fig. 6: The effect of MT on DPN rats

Notes: A: Schematic diagram of the animal experiment; B: Body weight and blood glucose levels of rats in each group (n = 6); C: Pathological examination of sciatic nerve tissues; D: Sciatic nerve conduction velocity (n = 6); E: Detection results of ROS levels (n = 6); F: Detection results of CHOP, PERK, IL-6, and TNF-α(n = 6); G: Immunohistochemical detection of positive expression of COX2 and IRE1α(n = 6). ***P*<0.01, ****P*<0.001 *vs.* the Control group; #*P*<0.05, ##*P*<0.01, ###*P*<0.001 *vs.* the Model group.

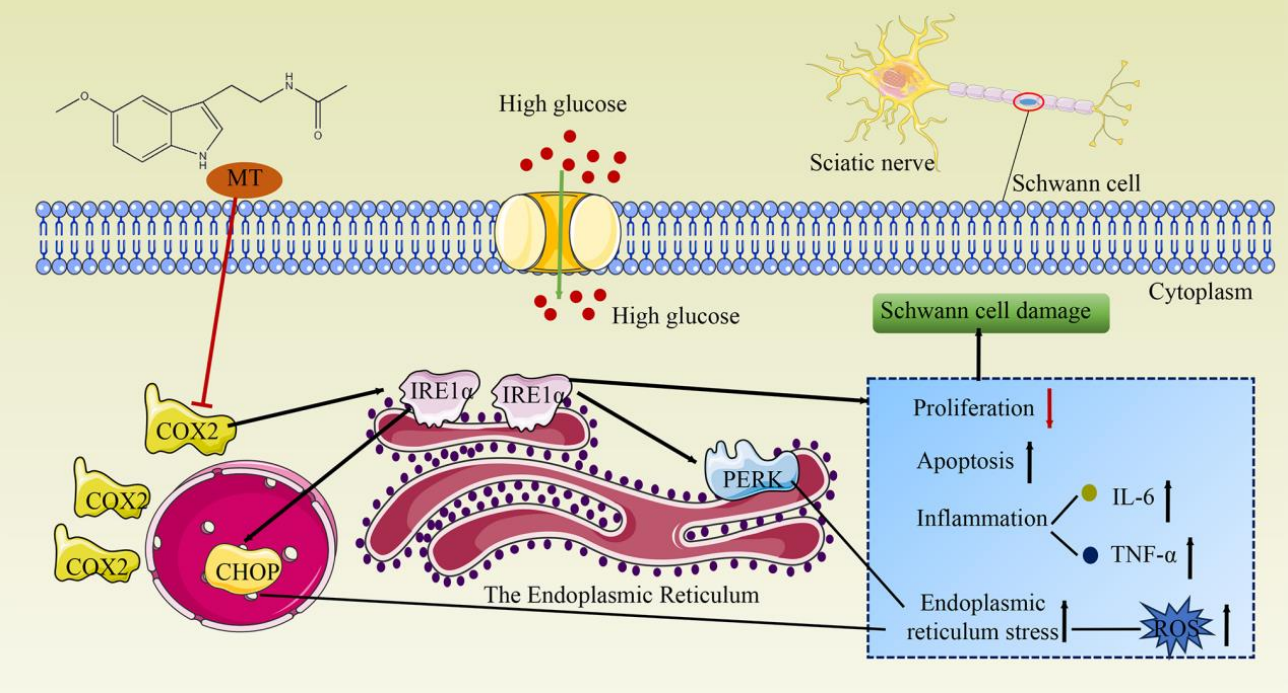

Fig. 7: Schematic diagram of the molecular mechanism by which MT improves DPN progression through the COX2/IRE1α axis by alleviating ER stress

Hyperglycemia has adverse effects on peripheral nervous system cells, including Schwann cells, triggering a series of pathological changes, such as excessive ROS production, exacerbated ER stress, and the release of pro-inflammatory factors. These pathological mechanisms substantially contribute to DPN progression (Bashir *et al.,* 2025; Callaghan *et al.,* 2020; Hu *et al.,* 2023). By detecting ER stress and inflammatory factors in RSC96 cells, this study found enhanced ER stress and inflammatory damage in HG-induced RSC96 cells. MT exhibited significant anti-ER stress and anti-inflammatory effects. Therefore, inhibiting ER stress and inflammatory damage is a potential strategy to improve DPN progression.

Notably, although the neuroprotective effects of MT in diabetic neuropathy have been widely reported, most previous studies have primarily attributed its benefits to its general antioxidant and anti-inflammatory properties (Kuthati *et al.,* 2025), without clearly identifying the specific upstream molecular pathways linking inflammation and ER stress. Tiong *et al.,* demonstrated that MT protects high-glucose-treated Schwann cells by reducing ROS, preserving mitochondrial membrane potential and inhibiting apoptosis (Tiong *et al.,* 2020). Salem *et al.,* showed that MT attenuates high-glucose-induced Schwann cell autophagy via the PERK-eIF2α-ATF4-CHOP branch of ER stress (Salem *et al.,* 2023). Previous studies have mainly focused on individual downstream pathways rather than the crosstalk between inflammation and ER stress. In contrast, suggests that COX2 may be an upstream melatonin-associated target and indicates, through gain- and loss-of-function experiments, that melatonin protects Schwann cells and sciatic nerve tissue by regulating the COX2/IRE1α axis, thereby linking inflammatory signaling to ER stress in DPN.

Through network pharmacology and bioinformatics analysis, this study identified COX2 as a molecular target of MT in the treatment of DPN. Western blot analysis revealed that MT could inhibit COX-2 expression. Previous studies have indicated that peony granules improve Schwann cell damage induced by HG and high fat by dampening ERK1/2 phosphorylation and COX2 expression and promoting the upregulation of SIRT2 (Shi *et al.,* 2024a). Other studies have also shown that cannabidiol and beta-caryophyllene can improve high-glucose-induced Schwann cell damage and inhibit COX2 activity (Khan *et al.,* 2024). Given the positive role of downregulating COX2 expression in the treatment of DPN in the aforementioned studies, this research examined the effects of COX2 overexpression on HG-induced RSC96 cells and found that COX2 overexpression could reverse the protective effects of MT. Cell growth was inhibited and ER stress and inflammatory damage were exacerbated. In addition, studies have found that the COX2 inhibitor celecoxib effectively inhibits IRE1α expression in the liver of cirrhotic rats, thereby reducing ER stress (Su *et al.,* 2020). Similarly, selective COX2 inhibitors can also alleviate ER stress in high-glucose-induced coronary endothelial cells by downregulating IRE1α levels (Haas *et al.,* 2022). In chronic diabetic neuropathy, protein kinase C epsilon (PKCε), an intracellular signaling molecule that

mediates chronic pain, is upregulated and is associated with ER stress-related molecules such as IRE1α (Kan *et al.,* 2024). Based on the above studies, it is hypothesized that the COX2/IRE1α axis may be an effective pathway for regulating ER stress in DPN. To verify this hypothesis, this study knocked down IRE1α and measured various indicators in each cell group. The results showed that knocking down IRE1α could reverse the damaging effects of COX2 overexpression on HG-induced RSC96 cells, promoting cell growth, reducing apoptosis and improving ER stress levels and inflammatory damage, thereby supporting the rationality of this hypothesis.

In animal experiments, MT significantly alleviated symptoms of nerve damage in DPN rats and effectively reduced ER stress in the sciatic nerve, accompanied by downregulation of COX2 and IRE1α expression. This was consistent with the protective effects of MT in the *in vitro DPN cell model involving* the COX2/IRE1α axis and provided a supportive basis for future clinical studies.

This study still has limitations. Although molecular docking and expression analyses suggested a potential interaction between melatonin and COX2, direct biochemical validation of target binding was not performed. In addition, our assessment of ER stress was limited to representative markers and did not include evaluation of the signaling cascade, such as XBP1 splicing or GRP78/BiP. Moreover, the *in-vitro* experiments were conducted in a single Schwann cell line, which may not fully capture the complexity of DPN pathophysiology. Finally, the animal experiment was constrained by a small sample size and lacked sensory behavioral assessment. Therefore, more rigorous mechanistic and functional validation is needed in future studies.

In summary, this study suggests the molecular mechanism by which MT improves DPN through ER stress regulation via the COX2/IRE1α axis (Fig. 7), providing a new research direction for the pharmacological treatment of DPN. However, research on this mechanism remains at the cellular and animal levels and further clinical trials are needed to verify its safety and efficacy.

Acknowledgements
This work was supported by the Major Science and Technology Special Plan of Yunnan Province (202102AA100061) and the Yunnan Clinical Research Center for Neurological Diseases (202505AJ310009).

Authors' contributions
Ansong Jin conceived the study and performed the statistical analysis. Leijing Ma contributed to the study design and data interpretation. Ansong Jin and Leijing Ma drafted the manuscript. All authors critically revised the manuscript for important intellectual content and approved the final version.

Funding
This work was supported by the Major Science and Technology Special Plan of Yunnan Province (202102AA100061) and the Yunnan Clinical Research Center for Neurological Diseases (202505AJ310009).

Data availability statement
The datasets analyzed in the current study are available from the corresponding author upon reasonable request.

Ethical approval
Approval for this research was granted by the Animal Experiment Ethics Committee of Kunming Medical University (Approval No. kmmu20211525). This study was performed in adherence with the ARRIVE guidelines. See supplementary file for the ARRIVE checklist.

Conflict of interest
The authors declare no competing interests.

Supplementary data

REFERENCES

Bashir S, Faheem M, Alamoudi MK, Alnami A, Almehmadi KA, Khan AW and Almutairy B (2025). Pharmacological and computational investigations of isosteviol 16-oxime for attenuating streptozotocin-induced diabetic neuroinflammation utilizing rat as animal model. *Int Immunopharmacol*, **153**: 114506.

Belyy V, Zuazo-Gaztelu I, Alamban A, Ashkenazi A and Walter P (2022). Endoplasmic reticulum stress activates human IRE1α through reversible assembly of inactive dimers into small oligomers. *Elife*, **11**: e74342.

Callaghan BC, Gallagher G, Fridman V and Feldman EL (2020). Diabetic neuropathy: What does the future hold? *Diabetologia*, **63**(5): 891–897.

Chang MC and S and Yang (2023). Diabetic peripheral neuropathy essentials: A narrative review. *Ann Palliat Med*, **12**(2): 390–398.

Che H, Li H, Li Y, Wang YQ, Yang ZY, Wang RL and Wang LH (2020). Melatonin exerts neuroprotective effects by inhibiting neuronal pyroptosis and autophagy in STZ-induced diabetic mice. *Faseb j*, **34**(10): 14042–14054.

Chen X, Shi C, He M, Xiong S and Xia X (2023). Endoplasmic reticulum stress: Molecular mechanism and therapeutic targets. *Signal Transduct Target Ther*, **8**(1): 352.

De Almeida Chuffa LG, Seiva FRF, Silveira HS, Cesario RC, da Silva Tonon K, Simao VA, Zuccari DAPC and Reiter RJ (2024). Melatonin regulates endoplasmic reticulum stress in diverse pathophysiological contexts: A comprehensive mechanistic review. *J Cell Physiol*, **239**(11): e31383.

Eftekharpour E and Fernyhough P (2022). Oxidative stress and mitochondrial dysfunction associated with

peripheral neuropathy in type 1 diabetes. *Antioxid Redox Signal*, **37**(7-9): 578–596.

Elafros MA, Andersen H, Bennett DL, Savelieff MG, Viswanathan V, Callaghan BC and Feldman EL (2022). Towards prevention of diabetic peripheral neuropathy: Clinical presentation, pathogenesis and new treatments. *Lancet Neurol*, **21**(10): 922–936.

Espino J, Rodriguez AB and Pariente JA (2019). Melatonin and oxidative stress in the diabetic state: Clinical implications and potential therapeutic applications. *Curr Med Chem*, **26**(22): 4178–4190.

Feng H, Wu T, Chin J, Ding R, Long C, Wang G, Yan D, Ma X and Yue R (2025). Tangzu granule alleviate neuroinflammation in diabetic peripheral neuropathy by suppressing pyroptosis through P2X7R /NLRP3 signaling pathway. *J Ethnopharmacol*, **337**(Pt 1): 118792.

Fridman V, Elafros M, Eid S, Reynolds EL, McCray B, ans Callaghan BC (2026). Advances in the pathophysiology and treatment of diabetic peripheral neuropathy. *BMJ*, **392**: e081217.

Groenendyk J, Paskevicius T, Urra H, Viricel C, Wang K, Barakat K, Hetz C, Kurgan L, Agellon LB and Michalak M (2018). Cyclosporine A binding to COX-2 reveals a novel signaling pathway that activates the IRE1α unfolded protein response sensor. *Sci Rep*, **8**(1): 16678.

Haas MJ, Warda F, Bikkina P, Landicho MA, Kapadia P, Parekh S and Mooradian AD (2022). Differential effects of cyclooxygenase-2 (COX-2) inhibitors on endoplasmic reticulum (ER) stress in human coronary artery endothelial cells. *Vascul Pharmacol*, **142**: 106948.

Hagen KM and Ousman SS (2021). Aging and the immune response in diabetic peripheral neuropathy. *J Neuroimmunol*, **355**: 577574.

Hashemi Goradel N, Najafi M, Salehi E, Farhood B and Mortezaee K (2019). Cyclooxygenase-2 in cancer: A review. *J Cell Physiol*, **234**(5): 5683–5699.

Hu Y, Chen C, Liang Z, Liu T, Hu X, Wang G, Hu J, Xie X and Liu Z (2023). Compound Qiying Granules alleviates diabetic peripheral neuropathy by inhibiting endoplasmic reticulum stress and apoptosis. *Mol Med*, **29**(1): 98.

Jeyam A, McGurnaghan SJ, Blackbourn LAK, McKnight JM, Green F, Collier A, McKeigue PM, Colhoun HM and SDRNT1BIO Investigators. (2020). Diabetic neuropathy is a substantial burden in people with type 1 diabetes and is strongly associated with socioeconomic disadvantage: A population-representative study from scotland. *Diabetes Care*, **43**(4): 734–742.

Kan YY, Chang YS, Liao WC, Chao TN and Hsieh YL (2024). Roles of neuronal protein kinase Cε on endoplasmic reticulum stress and autophagic formation in diabetic neuropathy. *Mol Neurobiol*, **61**(5): 2481–2495.

Khan I, Kaur S, Rishi AK, Boire B, Aare M and Singh M (2024). Cannabidiol and beta-caryophyllene combination attenuates diabetic neuropathy by inhibiting NLRP3 inflammasome/NFκB through the AMPK/sirT3/Nrf2 axis. *Biomedicines*, **12**(7).

Kuthati Y, Rao VN, Mende LK and Wong CS (2025). Therapeutic potential of melatonin in management of diabetic mellitus and diabetic neuropathic pain: Underlying mechanisms, challenges and future perspectives. *J Formos Med Assoc*. pp.S0929-6646(25)00456-5.

Li J, Guan R and Pan L (2023). Mechanism of Schwann cells in diabetic peripheral neuropathy: A review. *Medicine (Baltimore)*, **102**(1): e32653.

Ocak O, Silan F and Sahin EM (2022). Melatonin receptor gene polymorphisms as a risk factor in patients with diabetic peripheral neuropathy. *Diabetes Metab Res Rev*, **38**(8): e3573.

Patel S, Pangarkar A, Mahajan S and Majumdar A (2023). Therapeutic potential of endoplasmic reticulum stress inhibitors in the treatment of diabetic peripheral neuropathy. *Metab Brain Dis*, **38**(6):1841–1856.

Perveen W, Ahsan H, Rameen Shahzad Fayyaz S, Zaif A, Paracha MA, Nuhmani S, Khan M and Alghadir AH (2024). Prevalence of peripheral neuropathy, amputation and quality of life in patients with diabetes mellitus. *Sci Rep*, **14**(1): 14430.

Pourhanifeh MH, Hosseinzadeh A, Dehdashtian E, Hemati K and Mehrzadi S (2020). Melatonin: New insights on its therapeutic properties in diabetic complications. *Diabetol Metab Syndr*, **12**(1): 30.

Salem HMA, Chok KC, Koh RY, Ng PY, Tiong YL and Chye SM (2023). Melatonin ameliorates high glucose-induced autophagy in Schwann cells. *Int J Biochem Mol Biol*, **14**(3): 25–31.

Selvarajah D, Kar D, Khunti K, Davies MJ, Scott AR, Walker J and Tesfaye S (2019). Diabetic peripheral neuropathy: advances in diagnosis and strategies for screening and early intervention. *Lancet Diabetes Endocrinol*, **7**(12): 938–948.

Shi Y, Li H, Lin Y, Wang S and Shen G (2024a). Effective constituents and protective effect of Mudan granules against Schwann cell injury. *J Ethnopharmacol*, **323**: 117692.

Shi Y, Li H, Lin Y, Wang S and Shen G (2024b). Effective constituents and protective effect of Mudan granules against Schwann cell injury. *J Ethnopharmacol*, **323**: 117692.

Shokri M, Sajedi F, Mohammadi Y and Mehrpooya M (2021). Adjuvant use of melatonin for relieving symptoms of painful diabetic neuropathy: Results of a randomized, double-blinded, controlled trial. *Eur J Clin Pharmacol*, **77**(11): 1649–1663.

Su W, Tai Y, Tang SH, Ye YT, Zhao C, Gao JH, Tuo BG and Tang CW (2020). Celecoxib attenuates hepatocyte apoptosis by inhibiting endoplasmic reticulum stress in thioacetamide-induced cirrhotic rats. *World J Gastroenterol*, **26**(28): 4094–4107.

Tian L, Yang M, Tu S, Chang K, Jiang H, Jiang Y, Ding L, Weng Z, Wang Y, Tan X, Zong C, Chen B, Dou X, Wang

X and Qi X (2024). Xiaoke Bitong capsule alleviates inflammatory impairment via inhibition of the TNF signaling pathway to against diabetic peripheral neuropathy. *Phytomedicine*, **132**: 155867.

Tiong YL, Ng KY, Koh RY, Ponnudurai G and Chye SM (2020). Melatonin promotes Schwann cell dedifferentiation and proliferation through the Ras/Raf/ERK and MAPK pathways and glial cell-derived neurotrophic factor expression. *Exp Ther Med*, **20**(5): 16.

Wang X, Huan Y, Li C, Cao H, Sun S, Lei L, Liu Q, Liu S, Ji W, Liu H, Huang K, Zhou J and Shen Z (2020). Diphenyl diselenide alleviates diabetic peripheral neuropathy in rats with streptozotocin-induced diabetes by modulating oxidative stress. *Biochem Pharmacol*, **182**: 114221.

Xu D, Liu L, Zhao Y, Yang L, Cheng J, Hua R, Zhang Z and Li Q (2020). Melatonin protects mouse testes from palmitic acid-induced lipotoxicity by attenuating oxidative stress and DNA damage in a SIRT1-dependent manner. *J Pineal Res*, **69**(4): e12690.

Yan N, Xu Z, Qu C and Zhang J (2021). Dimethyl fumarate improves cognitive deficits in chronic cerebral hypoperfusion rats by alleviating inflammation, oxidative stress and ferroptosis via NRF2/ARE/NF-κB signal pathway. *Int Immunopharmacol*, **98**: 107844.

Yao W, Yang X, Zhu J, Gao B, Shi H and Xu L (2018a). IRE1α siRNA relieves endoplasmic reticulum stress-induced apoptosis and alleviates diabetic peripheral neuropathy *in-vivo* and *in-vitro*. *Sci Rep*, **8**(1): 2579.

Yao W, Yang X, Zhu J, Gao B, Shi H and Xu L (2018b). IRE1α siRNA relieves endoplasmic reticulum stress-induced apoptosis and alleviates diabetic peripheral neuropathy *in-vivo* and *in-vitro*. *Sci Rep*, **8**(1): 2579.

Yu MX, Lei B, Song X, Huang YM, Ma XQ, Hao CX, Yang WH and Pan ML (2021). Compound XiongShao Capsule ameliorates streptozotocin-induced diabetic peripheral neuropathy in rats via inhibiting apoptosis, oxidative - nitrosative stress and advanced glycation end products. *J Ethnopharmacol*, **268**: 113560.

Yuan Q, Zhang X, Wei W, Zhao J, Wu Y, Zhao S, Zhu L, Wang P and Hao J (2022). Lycorine improves peripheral nerve function by promoting Schwann cell autophagy via AMPK pathway activation and MMP9 downregulation in diabetic peripheral neuropathy. *Pharmacol Res*, **175**: 105985.

Ziegler D (2023). Pathogenetic treatments for diabetic peripheral neuropathy. *Diabetes Res Clin Pract*, **206** (Suppl 1): 110764.